Available online at www.sciencedirect.com
SCIENCE DIRECT
Journal of Magnetic Resonance 179 (2006) 11–19
JMR Journal of Magnetic Resonance
www.elsevier.com/locate/jmr

Magnetization and spin–spin energy diffusion in the XY model: A diagrammatic approach

Daniel Greenbaum *

Department of Physics, Massachusetts Institute of Technology, Cambridge, MA 02139, USA

Received 29 August 2005; revised 12 October 2005
Available online 14 November 2005

Abstract

It is shown that the diagrammatic cluster expansion technique for equilibrium averages of spin operators may be straightforwardly extended to the calculation of time-dependent correlation functions of spin operators. We use this technique to calculate exactly the first two non-vanishing moments of the spin–spin and energy–energy correlation functions of the XY model with arbitrary couplings, in the long-wavelength, infinite temperature limit appropriate for spin diffusion. These moments are then used to estimate the magnetization and spin–spin energy diffusion coefficients of the model using a phenomenological theory of Redfield. Qualitative agreement is obtained with recent experiments measuring diffusion of dipolar energy in calcium fluoride.

PACS: 75.45.+j; 76.60.-k

Keywords: High-temperature spin dynamics; Spin diffusion; Correlation function; Moment method; Dipolar coupling, XY model

1. Introduction

Experimentally measured quantities in spin systems can often be expressed in terms of time-dependent correlation functions of spin operators [1,2]. A well-known example is the free induction decay lineshape in solids [3,4]. Another example is the rate of spin diffusion [5], the transport of magnetization or spin–spin energy by mutual flips of spin pairs having the same Zeeman splitting.

The calculation of time-dependent correlation functions can be challenging both because of the structure of typical Hamiltonians for spin–spin interactions and because of the non-trivial commutation properties of spin operators. Of particular difficulty is the analysis of correlation functions of more than two spin operators. These arise in studying the diffusion of spin–spin energy, a problem in which interest has been revived by recent experiments that directly observed the diffusion of magnetization and dipolar energy in calcium fluoride [6,7]. A phenomenological approach developed by de Gennes [8] and Redfield [9] to calculate spin diffusion coefficients based on the knowledge of the first few moments of the associated correlation functions agrees well with experiments on magnetization diffusion. However, because of the difficulty of calculating moments for systems with long-range interactions, such as calcium fluoride, this approach has not been used to study spin–spin energy diffusion in such systems, while magnetization diffusion has only been studied to lowest order in perturbation theory in the flip-flop (or XY) term of the Hamiltonian [10].

In this paper, we present a diagrammatic technique for calculating the moments of time-dependent correlation functions, allowing a simplified treatment of the type of problems mentioned above. This technique extends an approach originally developed for calculating static, equilibrium averages in spin systems [11–14]. The extension is based on the cancellation of disconnected diagrams, proved in Appendix B. This cancellation greatly reduces

* Present address: Department of Condensed Matter Physics, Weizmann Institute of Science, 76100 Rehovot, Israel; Fax: +972 8 934 6019.
E-mail address: daniel.greenbaum@weizmann.ac.il.

1090-7807/$ - see front matter © 2005 Elsevier Inc. All rights reserved.
doi:10.1016/j.jmr.2005.10.011

the number of diagrams one needs to consider, and constitutes the primary advantage of the method.

The method is illustrated through application to the XY model. This model was chosen because it contains the simplest Hamiltonian exhibiting the dynamics of spin diffusion—mutual flips of spin pairs. It is therefore expected to qualitatively reproduce the behavior of more complicated systems, such as dipolar-coupled spins in high field, for which the dynamics is governed by the spin-flip process. It is also useful for comparison to the perturbative limit [10]. We calculate the first two non-vanishing moments of the spin–spin and energy–energy correlation functions in this model for arbitrary couplings, at infinite temperature. The expressions are exact in the long-wavelength limit. From these moments, analytic expressions for the diffusion coefficients are obtained. Choosing the coupling constants in our calculation to be those of calcium fluoride gives numerical values in qualitative agreement with experiments, as shown in Table 1. The ratio we find for the diffusion coefficients of magnetization and spin–spin energy is, however, a few times smaller than experimentally measured [7]. This may be due to our not having considered the full dipolar interaction, or to the importance of coherences in the quantum state of the spin system [15], which would not be taken into account by the present approach.

Besides the moment method, other approaches have yielded spin–spin energy diffusion coefficients, such as non-equilibrium statistical mechanics[16] and classical simulations.[17] However, the assumptions and approximations involved were difficult to justify and gave results which were not in better agreement with the recent experiments than those found here. Another recent calculation [15] for dipolar interactions was limited to the first two orders of perturbation theory in the flip-flop (XY) interaction, and gave similar qualitative agreement with the experiments. The work presented here should therefore complement the previous studies.

2. Model

The XY-model for N spins on a rigid lattice is

$$\mathscr{H} = \sum_{i,j}^{N} B_{ij} I_i^+ I_j^-, \tag{1}$$

with B_{ij}=0.

The latin indices run over all lattice sites and the I_i^α are spin operators defined by their commutation relations $[I_i^\alpha, I_j^\beta] = \delta_{ij} I_i^\gamma$, where α, β, γ is any cyclic permutation of x, y, z. The $I_j^\pm \equiv I_j^x \pm i I_j^y$ are raising and lowering operators. The combination of operators, $I_i^+ I_j^-$, generates mutual flips of spin pairs which are responsible for the transport of magnetization and spin–spin energy (or heat). The coefficients B_{ij} $(i \neq j)$ are arbitrary. To make contact with dipolar coupled spins, we use

$$B_{ij}^{\mathrm{dip}} = \frac{\gamma^2 \hbar}{4} \frac{3\cos^2\theta_{ij} - 1}{r_{ij}^3}. \tag{2}$$

Here, γ is the nuclear gyromagnetic ratio, $\mathbf{r}_{ij}$ is the displacement between lattice sites i and j, and θ_{ij} is the angle between $\mathbf{r}_{ij}$ and the external magnetic field $\mathbf{B}_0$, which is taken to lie along the z-axis. We do not include the Zeeman energy in Eq. (1) as it may be eliminated by a unitary transformation to the rotating frame [1].

The full Hamiltonian for dipolar coupled spins in a strong magnetic field[1] contains an additional term $-2\sum_{i,j}^{N} B_{ij}^{\mathrm{dip}} I_i^z I_j^z$, which we ignore here as discussed above. A complementary approach which includes this term but is perturbative in Eq. (1) has been discussed earlier [15].

The quantities of physical interest are correlation functions of the form

$$c_S(k,t) = \frac{\langle S(-k,t) S(k,0) \rangle}{\langle S(-k,0) S(k,0) \rangle}, \tag{3}$$

where $S(k,t) = \sum_i e^{ikz_i} S_i(t)$ is a spin operator or product of spin operators in the Heisenberg representation, and k is

Table 1
Summary of the results for the dipolar coupled XY model obtained from the moment method, with recent experimental values for comparison

Moments	[001]	[111]	
$M_{\mathscr{M}}^{(2)}/k^2$ ($\times 10^{-7}$ cm^2/s^2)	−5.59	−2.21	
$M_{\mathscr{M}}^{(4)}/k^2$ ($\times 10^{3}$ cm^2/s^4)	1.56	0.130	
$M_{\mathscr{H}}^{(2)}/k^2$ ($\times 10^{-7}$ cm^2/s^2)	−2.80	−1.08	
$M_{\mathscr{H}}^{(4)}/k^2$ (cm^2/s^4)	76.2	28.4	
Results for Gaussian cutoff	[001]	[111]	D_{001}/D_{111}
$D_{\mathscr{M}}$ ($\times 10^{-12}$cm^2/s)	13.3	11.4	1.17
$D_{\mathscr{H}}$ ($\times 10^{-12}$cm^2/s)	21.2	8.4	2.5
Ratio $D_{\mathscr{H}}/D_{\mathscr{M}}$	1.59	0.74	
$T_{\mathscr{M}}$ ($\times 10^{-6}$ s)	13.4	35.8	
$T_{\mathscr{H}}$ ($\times 10^{-6}$ s)	42.8	43.8	
Experiments ([6,7])	[001]	[111]	D_{001}/D_{111}
$D_{\mathscr{M}}$ Ref. [6] ($\times 10^{-12}$ cm^2/s)	7.1 ± 0.5	5.3 ± 0.3	1.34 ± 0.12
$D_{\mathscr{H}}$ Ref. [7] ($\times 10^{-12}$ cm^2/s)	29 ± 3	33 ± 4	0.88 ± 0.14
Ratio $D_{\mathscr{H}}/D_{\mathscr{M}}$	4.1 ± 0.7	6.2 ± 1.1	

the magnitude of the wavevector, which points along the magnetic field axis. In the specific cases which we consider below, S_i is either the local magnetization, $S_i = -\gamma\hbar I_i$, or spin–spin energy, $S_i = \sum_{j,(j\neq i)} \mathscr{H}_{ij}$, at lattice site i. The angular brackets denote averaging over an equilibrium ensemble. For most NMR problems, including spin diffusion, it suffices to consider $T = \infty$, so that $\langle\cdots\rangle = \mathrm{tr}\{\cdots\}/\mathrm{tr}\{\mathbf{1}\}$. The extension to finite temperature is straightforward and will not be considered here.

Below we will be interested in the moments of the correlation function, Eq. (3). Expanding in Taylor series about $t = 0$, we obtain

$$c_S(t) = \sum_{n=0}^{\infty} \frac{1}{(2n)!} M_S^{(2n)} t^{2n}. \tag{4}$$

The even moments $M_S^{(2n)}$ are given by

$$M_S^{(2n)} = (-1)^n \left(\frac{1}{\hbar}\right)^{2n} \frac{\langle S(k,0)[\mathscr{H}, S(-k,0)]_{2n}\rangle}{\langle S(-k,0)S(k,0)\rangle}, \tag{5}$$

where $[A,B]_n \equiv [A,[A,[\ldots[A,B]\ldots]]]$, with A appearing n times. The sum in Eq. (4) involves only even powers of t because the odd moments are zero. These expressions may be derived by expanding $S(k,t) = \mathrm{e}^{\mathrm{i}\mathscr{H}t} S(k,0)\mathrm{e}^{-\mathrm{i}\mathscr{H}t}$ by the well-known formula $\mathrm{e}^{A} B \mathrm{e}^{-A} = \sum_{n=0}^{\infty} \frac{1}{n!}[A,B]_n$ and putting the result in Eq. (3).

Following Redfield [9], one can obtain an approximate value of the diffusion coefficient of S from the first two non-vanishing moments [18]

$$D_S = \frac{1}{k^2\tau_S} = \frac{1}{k^2}\sqrt{\frac{\alpha_4}{\alpha_2^3}\frac{(M^{(2)})^3}{M^{(4)}}}, \tag{6}$$

where α_2 and α_4 are certain phenomenological parameters. We show in the next section that each moment is proportional to k^2 at long wavelength, so that this expression for D_S is independent of k. Eq. (6) is obtained by matching the terms of Eq. (4) to a phenomenological decay function of the form $f_S(t) = g_S(t)\mathrm{e}^{-t/\tau_S}$, where $\tau_S = (k^2 D_S)^{-1}$ is the diffusion time. The cutoff function $g_S(t)$ is different from unity only at times short compared to the spin–spin correlation time, $T_S \equiv \hbar/\max(B_{ij})$, which is roughly the time required for a single spin flip, and is in principle determined by the microscopic dynamics.

The exact values of the parameters α_{2n} are related to the manner in which the cutoff function $g_S(t)$ vanishes at high frequency. For example, a Gaussian and step-function cutoff give

$$\alpha_{2n} = \begin{cases} \frac{(-1)^n(2n-2)!}{\sqrt{\pi}2^{2n-2}(n-1)!}, & g_S(\omega) = \mathrm{e}^{-\omega^2 T_S^2}, \\ \frac{(-1)^n 2}{\pi(2n-1)}, & g_S(\omega) = \Theta(T_S^{-1} - \omega). \end{cases} \tag{7}$$

Both values have the same order of magnitude. Here $g_S(\omega)$ is the Fourier transform of $g_S(t)$. Since the shape of the cutoff function is not determined within the phenomenological model, Eq. (6) can only be viewed as approximate. Nevertheless, this shape is not expected to be drastically different for the magnetization and spin–spin energy diffusion coefficients, and therefore their ratio can be expected to have a weaker dependence on cutoff.

3. Calculation of moments

In this section, we calculate the second and fourth moments of magnetization and spin–spin energy for the XY model. Since we are interested in the long-wavelength behavior, we Taylor expand the correlation function, Eq. (3), in k. This gives

$$\begin{aligned} c_S(k,t) &= \frac{\sum_{i,j} \mathrm{e}^{\mathrm{i}k(z_i - z_j)}\langle S_i(0)S_j(t)\rangle}{\sum_i \langle S_i(0)^2\rangle} \\ &\simeq 1 - \frac{k^2}{2}\frac{\sum_{i,j} z_{ij}^2 \langle S_i(0)S_j(t)\rangle}{\sum_i \langle S_i(0)^2\rangle} + \mathrm{O}(k^4), \end{aligned} \tag{8}$$

where $z_{ij} \equiv z_i - z_j$, and the terms odd in z_{ij} are zero. The $\mathrm{O}(k^4)$ term is safely neglected as the correlation $\langle S_i(0)\, S_j(t)$ is a rapidly decaying function of the distance $|\mathbf{r}_i - \mathbf{r}_j|$. It depends on products of the spin–spin couplings, B_{ij}, which are either short-ranged or, in the case of dipolar coupling, decay algebraically on a length scale of a few lattice spacings. We will demonstrate this explicitly for each moment. The wavelength, $\lambda = 2\pi/k$, is taken to be much longer than this decay scale. In the calcium fluoride experiments [6,7] it is at least 10^4 lattice spacings. Expanding the commutator in Eq. (5), we obtain

$$\begin{aligned} M_S^{(2n)} = \frac{(-1)^{n+1}k^2}{2\sum_i \langle S_i(0)^2\rangle} \sum_{i,j} z_{ij}^2 \sum_{m=0}^{2n} \binom{2n}{m} \\ (-1)^m \langle \mathscr{H}^m S_j(0) \mathscr{H}^{2n-m} S_i(0)\rangle, \end{aligned} \tag{9}$$

for $n \geqslant 1$. Here $\binom{2n}{m} = \frac{(2n)!}{m!(2n-m)!}$ is a binomial coefficient, and we have used

$$[\mathscr{H}, S_j(0)]_{2n} = \sum_{m=0}^{2n} \binom{2n}{m} (-1)^m \mathscr{H}^m S_j(0) \mathscr{H}^{2n-m}. \tag{10}$$

Eq. (9) proves the k^2 dependence mentioned in the last section.

To calculate the moments for the XY model from Eq. (9), one must evaluate averages of the form $\langle \mathscr{H}^m S_j(0) \mathscr{H}^{2n-m} S_i(0)\rangle$. We do this using a diagrammatic cluster-expansion technique [11–14,2], extended to Eq. (9) with the help of a theorem proved in Appendix B. This technique eliminates the need for keeping track of the Kronecker deltas that arise from the contractions of spin operators, and allows the identification of the most important contributions to Eq. (9) at each n. It is based on an ordered cumulant expansion of spin operator averages. For completeness, a brief introduction to ordered cumulants of spin operators, also known as semi-invariants [11–14,2], is given in Appendix A.

3.1. Magnetization moments

Let $S_i = -\gamma\hbar I_i^z$, and consider the expression,

$$T_{2n} = (-1)^{n+1} \sum_{i,j} z_{ij}^2 \sum_{m=0}^{2n} \binom{2n}{m} (-1)^m \langle \mathscr{H}^m I_j^z \mathscr{H}^{2n-m} I_i^z \rangle, \tag{11}$$

in the numerator of Eq. (9). A diagram element is associated to each operator in this expression as follows:

$$I_i^z \longrightarrow \odot \tag{12}$$

$$\mathcal{H} = \sum_{kl} B_{kl} I_k^+ I_l^- \longrightarrow \overset{k}{\underset{l}{\downarrow}} \tag{13}$$

The indices k, l are dummies that are summed over, and in practice can be left off of diagrams. One then forms all possible topologically distinct, connected diagrams from these elements by joining them end-to-end in all possible ways, with the open circles for I^z inserted at vertices. The diagram elements are numbered based on the order in which they appear in Eq. (11). This order must be kept track of because of the non-trivial commutation properties of spin operators. For example, the diagrams corresponding to $\langle I_i^z \mathscr{H} I_j^z \mathscr{H} \mathscr{H} \mathscr{H} \rangle$ are numbered as follows:

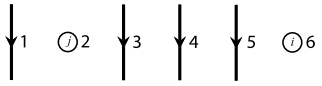

Each vertex without a circle is assigned a dummy summation index, and each vertex with a circle receives the index corresponding to that circle. The circles corresponding to i and j must appear at different vertices, since the z_{ij}^2 factor in Eq. (11) ensures that $i \neq j$. To each vertex is assigned an ordered cumulant. Each interaction line has an interaction coefficient associated with it that has the appropriate indices. For example, the line $k \longrightarrow l$ receives a factor of B_{kl}. The analytic expression corresponding to a given diagram is formed by taking the product of all the ordered cumulants and interaction coefficients associated with it, and summing over all dummy indices without restriction. The sum includes a factor of z_{ij}^2 and the appropriate binomial coefficients appearing in Eq. (11).

Of the total set of possible diagrams, many do not contribute. There are no diagrams with free ends, as these represent uncontracted spin operators which cause the trace to vanish. Each vertex must have the same number of lines leaving as entering, since all ordered cumulants with an unequal number of raising and lowering operators are zero. Finally, the disconnected diagrams vanish, as shown in Appendix B.

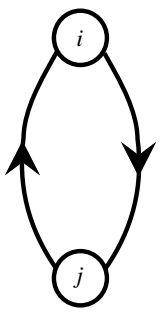

Fig. 1. Diagram contributing to second moment for magnetization.

The only diagram contributing to the second moment is shown in Fig. 1. Its contribution to Eq. (11) is

$$T_2 = \sum_{ij} z_{ij}^2 \sum_{m=0}^{2} \binom{2}{m} (-1)^m \times \overset{4}{\underset{m}{\circ}}$$

$$= \sum_{ij} z_{ij}^2 \times \left[1 \times \left({}_2\overset{4}{\circ}{}_3 + {}_3\overset{4}{\circ}{}_2 \right) - 2 \times \left({}_1\overset{4}{\circ}{}_3 + {}_3\overset{4}{\circ}{}_1 \right) + 1 \times \left({}_2\overset{4}{\circ}{}_1 + {}_1\overset{4}{\circ}{}_2 \right) \right]$$

$$= \sum_{ij} z_{ij}^2 B_{ij}^2 \Big[\Big(\langle\langle z+- \rangle\rangle \langle\langle -+z \rangle\rangle + \langle\langle z-+ \rangle\rangle \langle\langle +-z \rangle\rangle \Big)$$

$$-2 \Big(\langle\langle +z- \rangle\rangle \langle\langle -+z \rangle\rangle + \langle\langle -z+ \rangle\rangle \langle\langle +-z \rangle\rangle \Big)$$

$$+ \Big(\langle\langle -+z \rangle\rangle \langle\langle +-z \rangle\rangle + \langle\langle +-z \rangle\rangle \langle\langle -+z \rangle\rangle \Big) \Big]$$

$$= -\frac{1}{2} \sum_{ij} z_{ij}^2 B_{ij}^2. \tag{14}$$

The values of the ordered cumulants are $\langle\langle +-z \rangle\rangle = \frac{1}{4}$ and $\langle\langle -+z \rangle\rangle = -\frac{1}{4}$, as given in Table 2.

The denominator of Eq. (9) may be calculated without diagrams, and we obtain

$$\sum_i \langle (I_i^z)^2 \rangle = \frac{N}{4}. \tag{15}$$

Inserting these results into Eq. (9) gives

$$M_{\mathscr{M}}^{(2)} = -k^2 \sum_i z_{ik}^2 B_{ik}^2. \tag{16}$$

We note that, because of translational invariance, we can drop the summation over the dummy index k.

The diagrams contributing to the fourth moment for magnetization are shown in Fig. 2. They are calculated in

Table 2
Ordered Cumulants for spin 1/2 and $T = \infty$

$\langle\langle z \rangle\rangle = 0$	$\langle\langle +-+-z \rangle\rangle = 0$
$\langle\langle zz \rangle\rangle = \frac{1}{4}$	$\langle\langle -++-z \rangle\rangle = 0$
$\langle\langle +- \rangle\rangle = \frac{1}{2}$	$\langle\langle +--+z \rangle\rangle = 0$
$\langle\langle +-z \rangle\rangle = \frac{1}{4}$	$\langle\langle ++--z \rangle\rangle = -\frac{1}{2}$
$\langle\langle -+z \rangle\rangle = -\frac{1}{4}$	$\langle\langle --++z \rangle\rangle = \frac{1}{2}$
$\langle\langle zzz \rangle\rangle = 0$	$\langle\langle -+-+z \rangle\rangle = 0$
$\langle\langle zzzz \rangle\rangle = -\frac{1}{8}$	$\langle\langle +++--- \rangle\rangle = \frac{3}{2}$
$\langle\langle +-zz \rangle\rangle = 0$	$\langle\langle ++-+-- \rangle\rangle = \frac{1}{2}$
$\langle\langle +z-z \rangle\rangle = -\frac{1}{4}$	$\langle\langle ++--+- \rangle\rangle = \frac{1}{2}$
$\langle\langle +-+- \rangle\rangle = \frac{1}{2}$	$\langle\langle +-+-+- \rangle\rangle = \frac{1}{2}$
$\langle\langle ++-- \rangle\rangle = -\frac{1}{2}$	

We use the shorthand notation + for I^+, − for I^-, and z for I^z. Cumulants that do not have the same number of raising and lowering operators are zero, and are not included. We also include only one of each set of cumulants that differ by a cyclic permutation of its operators. As discussed in the text, these cumulants are the same at $T = \infty$.

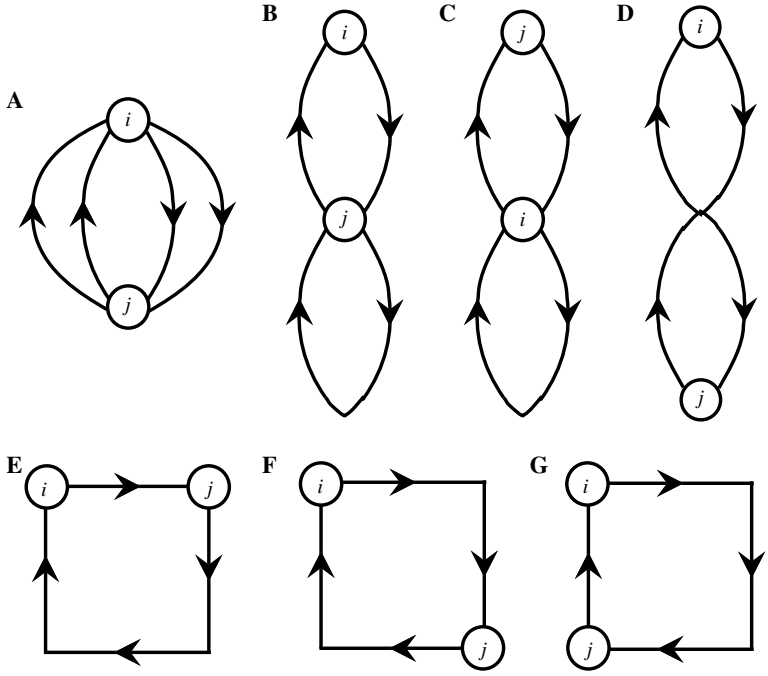

Fig. 2. All topologically distinct diagrams containing two circles and four interaction lines. The diagrams shown here arise in the calculation of the fourth moment for magnetization as well as that of the second moment for spin–spin energy. The analytic expressions for the diagrams are different in the two cases, however.

a similar way to those for the second moment, so we omit the details. Table 2 shows that most of the fourth and fifth-order cumulants are zero, which enables us to consider only a subset of the orderings of the diagram elements. The non-zero cumulants at fourth and fifth order correspond to vertices with two ingoing and two outgoing lines, with both ingoing lines next to each other in the order (same for the outgoing lines). The calculation shows that only the diagrams labelled A–C in Fig. 2 contribute. The fourth moment is

$$M_{\mathscr{M}}^{(4)} = -4k^2\left[\sum_i z_{ik}^2 B_{ik}^4 - \left(\sum_i z_{ik}^2 B_{ik}^2\right)\left(\sum_i B_{ik}^2\right)\right]. \tag{17}$$

3.2. Energy moments

The expression in the numerator of Eq. (9) for spin–spin energy, corresponding to Eq. (11), is

$$T_{2n} = (-1)^{n+1}\sum_{i,j,k,l} z_{ij}^2 \sum_{m=0}^{2n}\binom{2n}{m}(-1)^m\langle \mathscr{H}^m \mathscr{H}_{jl}\mathscr{H}^{2n-m}\mathscr{H}_{ik}\rangle, \tag{18}$$

where $S_i = \sum_{k,(k\neq i)}\mathscr{H}_{ik}$, and:

$$\mathscr{H}_{ik} = \mathscr{H}_{ik}^{(+)} + \mathscr{H}_{ik}^{(-)}, \tag{19}$$

$$\mathscr{H}_{ik}^{(+)} \equiv \frac{1}{2}B_{ik}I_i^+ I_k^-, \tag{20}$$

$$\mathscr{H}_{ik}^{(-)} \equiv \frac{1}{2}B_{ik}I_i^- I_k^+. \tag{21}$$

We can rewrite Eq. (18) as:

$$T_{2n} = 2\left(T_{2n}^{(+)} + T_{2n}^{(-)}\right), \tag{22}$$

$$T_{2n}^{(+)} \equiv \sum_{i,j,k,l} z_{ij}^2 \sum_{m=0}^{2n}\binom{2n}{m}(-1)^{(n+m+1)} \langle \mathscr{H}^m \mathscr{H}_{jl}^{(+)}\mathscr{H}^{2n-m}\mathscr{H}_{ik}^{(+)}\rangle, \tag{23}$$

$$T_{2n}^{(-)} \equiv \sum_{i,j,k,l} z_{ij}^2 \sum_{m=0}^{2n}\binom{2n}{m}(-1)^{(n+m+1)} \langle \mathscr{H}^m \mathscr{H}_{jl}^{(+)}\mathscr{H}^{2n-m}\mathscr{H}_{ik}^{(-)}\rangle, \tag{24}$$

where use has been made of the formula

$$\langle (A + A^\dagger)(B + B^\dagger)\rangle = 2\mathrm{Re}\langle (A + A^\dagger)B\rangle, \tag{25}$$

for any operators A and B.

We associate the following diagram elements with the operators appearing in Eqs. (23) and (24).

$\mathscr{H}_{ik}^{(+)} \longrightarrow$  (26)

$\mathscr{H}_{ik}^{(-)} \longrightarrow$  (27)

The diagram element for the full interaction, $\mathscr{H}$, is the same as in the last section, i.e., Eq. (13). Dummy indices such as k will be left off of the diagrams as before.

The calculation of Eq. (18) is similar to that of Eq. (11). In this case, however, the interaction lines due to $\mathscr{H}_{ik}^{(+)}$ and $\mathscr{H}_{ik}^{(-)}$ receive an additional factor of $\frac{1}{2}$, because this factor

appears in Eqs. (20) and (21). The final result is multiplied by the factor 2 appearing in Eq. (22).

The diagrams contributing to the second moment for spin–spin energy are shown in Fig. 2. These diagrams are exactly the same as the ones arising in the calculation of the fourth moment for magnetization. However, their meaning is different, as now there are no I^z operators, and we deal with a different set of ordered cumulants. We note that the diagrams at order $(2n)$ for spin–spin energy are always the same as those at order $(2n+2)$ for magnetization.

One can easily see that the diagrams labelled E–G in Figs. 2 are zero. Associated with each of them is the product of ordered cumulants, $\langle\langle +- \rangle\rangle^4 = \frac{1}{16}$. Because this cumulant factor is the same regardless of the order of diagram elements, we can move all the diagrams to the left of the second summation sign in Eq. (18). For example, diagram (E) gives

$$T_2(e) = 2\sum_{ij} z_{ij}^2 \sum_{m=0}^{2} \binom{2}{m} (-1)^m \times \quad = 2\sum_{ij} z_{ij}^2 \times \quad \times \sum_{m=0}^{2} \binom{2}{m} (-1)^m. \tag{28}$$

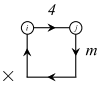

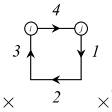

Since the sum over binomial coefficients is zero, we have $T_2(e) = 0$.

By direct calculation, it is also easily found that the diagrams labelled (A–C) are zero. The only diagram contributing to the second moment for spin–spin energy is therefore diagram (D) of Fig. 2. Eq. (18) then reads

$$T_2 = 2\sum_{ij} z_{ij}^2 \sum_{m=0}^{2} \binom{2}{m} (-1)^m \times \tag{29}$$

According to Table 2, $\langle\langle +-+- \rangle\rangle = 0$. This restricts the possible orderings of the diagram elements, since not all vertices with four lines are allowed. Therefore

$$T_2 = 2\sum_{ij} z_{ij}^2 \times \tag{30}$$

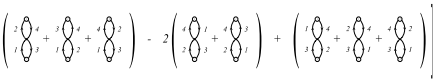

The product of ordered cumulants is the same for each diagram in Eq. (30). It is $\langle\langle +- \rangle\rangle^2 \langle\langle ++-- \rangle\rangle = (\frac{1}{2})^2(-\frac{1}{2}) = -\frac{1}{8}$. Multiplying by $\frac{1}{4}$ for the two circles, we obtain

$$T_2 = 2\left(-\frac{1}{8}\right)\left(\frac{1}{4}\right)\sum_{ijk} z_{ij}^2 B_{ik}^2 B_{jk}^2 \times [1(3) - 2(2) + 1(3)] = -\frac{1}{8}\sum_{ijk} z_{ij}^2 B_{ik}^2 B_{jk}^2. \tag{31}$$

The denominator of Eq. (9) is given by $\langle\langle +- \rangle\rangle^2 \sum_{ij} B_{ij}^2 = \frac{1}{4}\sum_{ij} B_{ij}^2$. Inserting these results into Eq. (9), we obtain

$$M_{\mathscr{H}}^{(2)} = -\frac{k^2}{4}\frac{\sum_{ij} z_{ik}^2 B_{ij}^2 B_{jk}^2}{\sum_i B_{ik}^2}, \tag{32}$$

where we have used translational invariance to drop one of the summations.

The types of diagrams arising in the calculation of the fourth moment are shown in Fig. 3. To save space, the distinct topologies are pictured without circles. The entire set of diagrams at fourth order is obtained by placing two circles at the vertices of the diagrams in Fig. 3 in all possible ways. The result is straightforward to calculate, and is

$$\begin{aligned} M_{\mathscr{H}}^{(4)} = {} & k^2 \sum_{ij} z_{ik}^2 B_{ik}^2 B_{jk}^2 - 2k^2 \frac{\sum_{ij} z_{ik}^2 \left(B_{ik}^2 B_{jk}^4 + B_{ik}^4 B_{jk}^2\right)}{\sum_i B_{ik}^2} - \frac{9}{4}k^2 \\ & \times \frac{\sum_{ij} z_{ik}^2 B_{ik}^2 B_{jk}^2 B_{ij}^2}{\sum_i B_{ik}^2} - \frac{k^2}{4} \\ & \times \frac{\sum_{ijl} z_{ik}^2 \left(6B_{ik}^2 B_{jk} B_{kl} B_{ij} B_{il} - 18 B_{ik} B_{jk}^2 B_{kl} B_{ij} B_{jl} + 11 B_{jk} B_{kl} B_{ij} B_{il} B_{jl}^2\right)}{\sum_i B_{ik}^2}. \end{aligned} \tag{33}$$

The sums over the index k are left off, as usual. The first term in Eq. (33) comes from diagrams (A) and (B). Diagram (C) is of the same order of magnitude, and gives the second term in this equation. Diagrams (D) and (E) give rise to the third term, and are an order of magnitude smaller for short-ranged or dipolar coupling. Diagrams (G–I) give the last term in Eq. (33) and are another order of magnitude smaller. The general guidelines are that those diagrams with the greatest number of lines per pair of vertices are the largest. The ones with several pairs of vertices joined by only a single line, such as diagrams (G–I), are the smallest. There are exceptions to these guidelines (For example, diagram (F) vanishes, for the same reason as does the corresponding diagram at second order.), so care must be taken in their application. As for the second moment, the diagrams (L) vanish, as do diagrams (J) and (K).

4. Numerical results for dipolar-coupled XY model

The results of numerical evaluation of the moments calculated in the last section for $B_{ij} = B_{ij}^{\mathrm{dip}}$ (see Eq. (2)), are given in Table 1. This corresponds to dipolar coupling. We have used values of the gyromagnetic ratio and lattice spacing for the fluorines in calcium fluoride of $\gamma = 2.51 \times 10^4$ rad s^{-1} Oe^{-1} and $a = 2.73 \times 10^{-8}$ cm. Because lattice sums can be evaluated numerically only for finite lattice sizes, we used finite size scaling to extract the infinite lattice limit. The approach to the infinite lattice value is expected to follow a power law. For example, if we approximate the sums by integrals in Eq. (16),

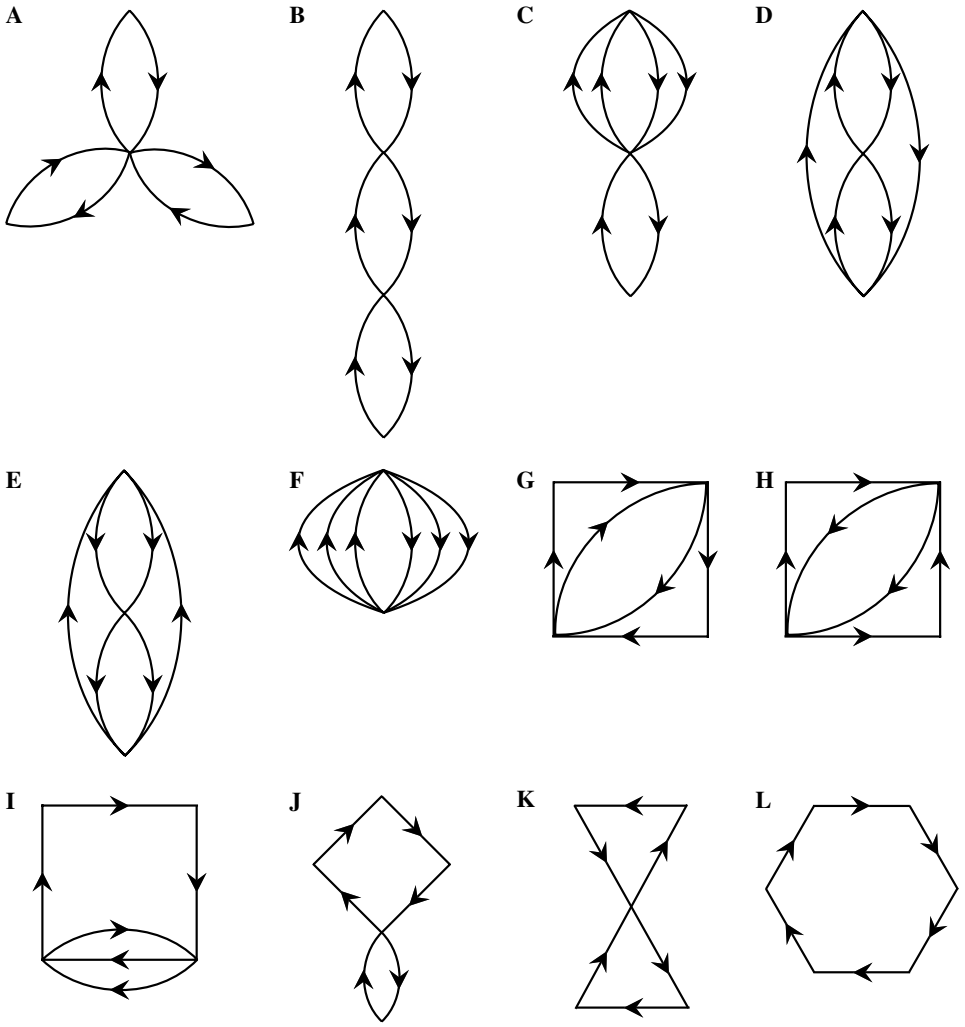

Fig. 3. All topologically distinct diagrams containing six interaction lines. Diagrams for the fourth energy moment are obtained by placing circles with indices i and j at vertices in all distinct ways.

$$M_{\mathscr{M}}^{(2)} \approx -k^2 \int_{a\leqslant r\leqslant L} \mathrm{d}^3\mathbf{r} B^{\mathrm{dip}}(\mathbf{r})^2 z^2 \sim \text{const} \times \int_a^L r^2 \mathrm{d}r \left(\frac{1}{r^3}\right)^2 r^2 = \text{const} \times \left(\frac{1}{a} - \frac{1}{L}\right). \quad (34)$$

We performed a least squares fit to a power law of the quantities in Eqs. (16), (17), (32), and (33) as a function of lattice size, for both the [0 0 1] and [1 1 1] orientations of the crystal with respect to the external field. We found it sufficient to vary the lattice size between 1 and 81 lattice sites on an edge, in increments of 2 lattice sites. This gave agreement with Eq. (34) to better than one percent. The numbers in Table 1 are the infinite lattice values extracted from the scaling analysis.

Besides the moments, Table 1 gives the values for the diffusion coefficients for both Gaussian and step-function cutoff (see Eq. (7)), as well as their ratio. We find fair agreement with experiments on calcium fluoride for the magnitudes of both diffusion coefficients. For magnetization, our value is slightly high, while for spin–spin energy it is slightly low. The ratio $D_{\mathscr{H}}/D_{\mathscr{M}}$ that we calculate is about 1.6 for the [0 0 1] direction, while in these experiments it is between 4 and 6. Given the phenomenological nature of the theory we feel this to be adequate agreement. For the [1 1 1] direction, the results are quite different, giving a ratio of diffusion coefficients that is less than one. We cannot account for this difference but conjecture that it may be the result of neglecting the Ising, or $I^z I^z$, term from the calculation.

As an additional check for consistency of this theory we have calculated the value of the short time cutoff, T_S, using its relation[10] to the moments of the appropriate cutoff function in Eq. (7). As Table 1 shows, T_S was found to be on the order of 10–100 μs for the different cutoff functions and crystal orientations that we considered. This is consistent with the assumption that T_S is related to the spin–spin correlation time given by the free induction decay. The timescale associated with this decay in calcium fluoride is approximately 20 μs with the external field in the [0 0 1] direction and approximately 50 μs with the external field in the [1 1 1] direction [4].

5. Conclusion

We have shown how the diagrammatic technique for calculating equilibrium correlation functions in spin systems may be adapted to the evaluation of multi-spin dynamical correlation functions. We used this technique to obtain exactly the first two non-vanishing moments of the magnetization and spin–spin energy autocorrelation functions of the XY model at infinite temperature and long wavelength. The results were used to estimate the magnetization and spin–spin energy diffusion coefficients in the case of dipolar coupling, using a phenomenological moment method. We found qualitative agreement with experiments on calcium fluoride for both diffusion coefficients. The ratio of the diffusion coefficient for spin–spin energy to that for magnetization was found to be greater than one for the [0 0 1] orientation of the external field with respect to the crystal axes. However, this is not large enough to accurately account for the observations. The orientation dependence of the diffusion coefficients was also in qualitative agreement for magnetization, but not for spin–spin energy. The lack of any experimentally observed orientation dependence for spin–spin energy diffusion leads us to conjecture that some additional, possibly k-dependent, decay processes may have been at play in the experiment, increasing the observed decay rates. Some artifacts of the coherent time evolution of the spin system could also have been involved, and would not be accounted for in the phenomenological model of irreversible decay that was used here. Finally, it is possible that the approximation of dropping the Ising (I^zI^z) term was too drastic. A tractable calculation including this term should be possible along the lines presented here. Although we focused here on the spin diffusion problem, the generality of the technique should allow for wider applicability.

Acknowledgments

I thank David Cory and Chandrasekhar Ramanathan for introducing me to the problem of spin diffusion and for their guidance in the early stages of this work. I would also like to acknowledge support from the NSF through a research assistantship at MIT and from a Feinberg Fellowship at the Weizmann Institute.

Appendix A. Ordered cumulants

Ordered cumulants are used to simplify the evaluation of averages of spin operators summed over the lattice. The non-zero elements of a spin operator average contain, in general, several operators with the same lattice site index. Since operators with different indices commute, we may rearrange them so that all operators with the same index are next to each other, and then factor the average into averages over operators at different lattice sites, since traces at different lattice sites are independent. For example, $\langle I_k^+ I_i^z I_k^- I_i^z\rangle = \langle I_k^+ I_k^-\rangle\langle I_i^z I_i^z\rangle$ if $i \neq k$. Since we only consider a Hamiltonian that is invariant under lattice translations, the averages in the last expression are independent of index. A general spin operator average may be calculated by grouping the operators by index in this fashion, in all possible ways, taking care to avoid over-counting by not including identical groupings more than once. For example, $\sum_{ik} A_{ik}\langle I_i^+ I_k^-\rangle = \sum_{ik} A_{ik}[\delta_{ik}\langle I_i^+ I_i^-\rangle + (1-\delta_{ik})\langle I_i^+\rangle\langle I_k^-\rangle] = \sum_i A_{ii}(\langle I_i^+ I_i^-\rangle - \langle I_i^+\rangle\langle I_i^-\rangle) + \sum_{ik} A_{ik}\langle I_i^+\rangle\langle I_k^-\rangle$. Defining the ordered cumulants, $\langle\langle +-\rangle\rangle \equiv \langle I_i^+ I_i^-\rangle - \langle I_i^+\rangle\langle I_i^-\rangle$, $\langle\langle +\rangle\rangle \equiv \langle I_i^+\rangle$, and $\langle\langle -\rangle\rangle \equiv \langle I_i^-\rangle$, for an arbitrary index i, we obtain $\sum_{ik} A_{ik}\langle I_i^+ I_k^-\rangle = \langle\langle +-\rangle\rangle\sum_i A_{ii} + \langle\langle +\rangle\rangle\langle\langle -\rangle\rangle\sum_{ik} A_{ik}$.

Generalizing the above example, we define ordered cumulants, also known as semi-invariants,[2,11–14] iteratively in terms of their factorization in cumulants of lower degree. Thus:

$$
\begin{aligned}
&\langle\langle +\rangle\rangle = \langle I^+\rangle,\\
&\langle\langle -\rangle\rangle = \langle I^-\rangle,\\
&\langle\langle z\rangle\rangle = \langle I^z\rangle,\\
&\langle\langle I^z I^+\rangle\rangle = \langle I^z I^+\rangle - \langle\langle I^z\rangle\rangle\langle\langle I^+\rangle\rangle,\\
&\langle\langle I^z I^-\rangle\rangle = \langle I^z I^-\rangle - \langle\langle I^z\rangle\rangle\langle\langle I^-\rangle\rangle,\\
&\langle\langle I^+ I^-\rangle\rangle = \langle I^+ I^-\rangle - \langle\langle I^+\rangle\rangle\langle\langle I^-\rangle\rangle,\\
&\langle\langle I^z I^+ I^-\rangle\rangle = \langle I^z I^+ I^-\rangle - \langle\langle I^z I^+\rangle\rangle\langle\langle I^-\rangle\rangle - \langle\langle I^z I^-\rangle\rangle\langle\langle I^+\rangle\rangle\\
&\qquad\qquad - \langle\langle I^+ I^-\rangle\rangle\langle\langle I^z\rangle\rangle - \langle\langle I^z\rangle\rangle\langle\langle I^+\rangle\rangle\langle\langle I^-\rangle\rangle,
\end{aligned}
\tag{A.1}
$$

and so on. Ordered cumulants are related to spin operator averages in an analogous way to the relation of cumulants and averages in probability theory. The main difference is that the order of the spin operators within the cumulant is important due to their non-trivial commutation relations. Using ordered cumulants, it is possible to calculate operator averages without restricting the summation indices, as shown in the preceding paragraph.

A list of ordered cumulants up to degree 5 for spin $\frac{1}{2}$ and $T = \infty$ is given in Table 2. We omit cumulants that differ only by a cyclic permutation of their operators. In the limit of infinite temperature in which we are interested, the density matrix is proportional to unity, and these cumulants are the same by the properties of the trace. We note that this cyclic invariance is not a general property at finite temperature. Besides cyclic permutations, cumulants differing by any other rearrangements in the order of the operators generally have different values even at infinite temperature. Finally, cumulants with unequal numbers of raising and lowering operators are zero and are not included in the table.

Appendix B. Cancellation of disconnected diagrams

We present a combinatorial proof of the cancellation of disconnected diagrams for the time-independent Hamiltonian, Eq. (1). To account for time dependence or an I^zI^z term, it is possible to proceed by the standard method via the interaction picture and S-matrix expan-

sion.[19] However, the inapplicability of Wick's theorem for spin operators prohibits the factorization of time-ordered products into contractions, and we must eventually use the same type of counting argument presented here.

Eq. (9) contains the term

$$\sum_{m=0}^{n}\binom{n}{m}(-1)^m\langle\mathscr{H}^{n-m}S_j\mathscr{H}^m S_i\rangle. \tag{B.1}$$

There are two types of disconnected diagrams which contribute to this term, those in which both S_j and S_i appear in the same cumulant, and those in which they belong to different cumulants. The latter type of disconnected diagram is always zero, because the cyclic permutation symmetry of the trace allows us to factor all the cumulants to the left of the summation over m in Eq. (B.1).

The case where both S_j and S_i appear in the same cumulant is slightly more involved. Consider the subset of diagrams for which $l<n$ interaction lines form the part which is not connected to that containing S_j and S_i. The l interaction lines can correspond to any of the $n\mathscr{H}$'s appearing in Eq. (B.1), whose average may be factored outside the summation over m. Depending on which ones we choose to factor out, there will be a different number of $\mathscr{H}$'s to the right of the operator S_j. If we choose to leave $k\leq n\mathscr{H}$'s to the right of S_j, we can do this in $\binom{m}{m-k}\binom{n-m}{l-(m-k)}$ ways. The sum over m in Eq. (B.1) for the set of diagrams with $l\mathscr{H}$'s factored out is therefore equal to

$$\begin{aligned}&\sum_{m=0}^{n}\binom{n}{m}(-1)^m\langle\mathscr{H}^{n-m}S_j\mathscr{H}^m S_i\rangle\\&\quad=\langle\mathscr{H}^l\rangle\sum_{k=0}^{n-l}\langle\mathscr{H}^{n-l-k}S_j\mathscr{H}^k A_2\rangle\times\sum_{m=k}^{l+k}(-1)^m\binom{n}{m}\\&\qquad\times\binom{m}{m-k}\binom{n-m}{l-(m-k)}.\end{aligned} \tag{B.2}$$

The product of binomial coefficients in this equation is

$$\begin{aligned}&\binom{n}{m}\binom{m}{m-k}\binom{n-m}{l-(m-k)}\\&\quad=\frac{n!m!(n-m)!}{(n-m)!m!(m-k)!k!(l+k-m)!(n-l-k)!}\\&\quad=\frac{n!}{(m-k)!k!(l+k-m)!(n-l-k)!}.\end{aligned} \tag{B.3}$$

The only factors that depend on m are $\frac{1}{(m-k)!(l+k-m)!}=\frac{1}{l!}\binom{l}{m-k}$. The sum over m in Eq. (B.2) is therefore $\sum_{m=k}^{l+k}(-1)^m\binom{l}{m-k}=0$. This proves the vanishing of disconnected diagrams.

References

[1] A. Abragam, The Principles of Nuclear Magnetism, Oxford University Press, Oxford, 1961.
[2] A. Abragam, M. Goldman, Nuclear Magnetism: Order and Disorder, Clarendon Press, Oxford, 1982.
[3] J.H. Van Vleck, The dipolar broadening of magnetic resonance lines in crystals, Phys. Rev. 74 (1948) 1168–1183.
[4] I.J. Lowe, R.E. Norberg, Free-induction decays in solids, Phys. Rev. 107 (1957) 46–61.
[5] N. Bloembergen, On the interaction of nuclear spins in a crystalline lattice, Physica 15 (1949) 386–426.
[6] W. Zhang, D.G. Cory, First direct measurement of the spin diffusion rate in a homogenous solid, Phys. Rev. Lett. 80 (1998) 1324–1327.
[7] G.S. Boutis, D. Greenbaum, H. Cho, D.G. Cory, C. Ramanathan, Spin diffusion of correlated two-spin states in a dielectric crystal, Phys. Rev. Lett. 92 (2004) 137201.
[8] P.G. de Gennes, J. Phys. Chem. Solids 7 (1958) 345.
[9] A.G. Redfield, Spatial diffusion of spin energy, Phys. Rev. 116 (1959) 315–316.
[10] A.G. Redfield, W.N. Yu, Moment-method calculation of magnetization and interspin-energy diffusion, Phys. Rev. 169 (1968) 443–450, 177 (1969) 1018.
[11] R. Brout, Statistical mechanical theory of a random ferromagnetic system, Phys. Rev. 115 (1959) 824–835.
[12] R. Brout, Statistical mechanical theory of ferromagnetism. high density behavior, Phys. Rev. 118 (1960) 1009–1019.
[13] F. Englert, Linked cluster expansions in the statistical theory of ferromagnetism, Phys. Rev. 129 (1963) 567–577.
[14] R.B. Stinchcombe, G. Horwitz, F. Englert, R. Brout, Thermodynamic behavior of the heisenberg ferromagnet, Phys. Rev. 130 (1963) 155–176.
[15] D. Greenbaum, M. Kindermann, C. Ramanathan, D.G. Cory, Hydrodynamic approach to coherent nuclear-spin transport, Phys. Rev. B 71 (2005) 054403.
[16] W. Walgraef, P. Borckmans, Spin and interspin energy diffusion coefficients, Physica 68 (1973) 157–163.
[17] C. Tang, J.S. Waugh, Dynamics of classical spins on a lattice: spin diffusion, Phys. Rev. B. 45 (1992) 748–754.
[18] The truncated Lorentzian leading to Eq. (6) has also been used in the theory of resonance lineshapes in solids. The underlying physical assumption is the same in both cases, namely that correlations decay exponentially at long times and quadratically at short times. See, for instance [1], Chapter 3.
[19] M.E. Peskin, D.V. Schroeder, An Introduction to Quantum Field Theory, Perseus Books, 1995.